Flow field in shallow reservoir with varying inlet and outlet position

VELIA FERRARA, PhD student, *Hydraulics in Environmental and Civil Engineering (HECE), Research unit Urban & Environmental Engineering, University of Liege (ULg), Liege, Belgium*

Email: velya@hotmail.it

SÉBASTIEN ERPICUM (IAHR Member), Assistant Professor , *Hydraulics in Environmental and Civil Engineering (HECE), Research unit Urban & Environmental Engineering, University of Liege (ULg), Liege, Belgium*

Email: s.erpicum@ulg.ac.be

PIERRE ARCHAMBEAU, Research Associate, *Hydraulics in Environmental and Civil Engineering (HECE), Research unit Urban & Environmental Engineering, University of Liege (ULg), Liege, Belgium*

Email: pierre.archambeau@ulg.ac.be

MICHEL PIROTTON, Full Professor, *Hydraulics in Environmental and Civil Engineering (HECE), Research unit Urban & Environmental Engineering, University of Liege (ULg), Liege, Belgium*

Email: michel.pirotton@ulg.ac.be

BENJAMIN DEWALS (IAHR Member), Associate Professor, *Hydraulics in Environmental and Civil Engineering (HECE), Research unit Urban & Environmental Engineering, University of Liege (ULg), Liege, Belgium*

Email: b.dewals@ulg.ac.be

Running Head: Flow field in shallow reservoir

Flow field in shallow reservoir with varying inlet and outlet position

ABSTRACT

Shallow reservoirs are used for multiple purposes, such as storm water retention and trapping of sediments. Reliable predictions of the flow fields are necessary to inform the design and operation of these structures. Using numerical simulations, we performed a systematic analysis of the influence of the location of the inlet and outlet on the flow fields developing in rectangular shallow reservoirs of various sizes. Depending on the relative location of the inlet and outlet with respect to the reservoir centreline, contrasting flow patterns are obtained, involving either no flow reattachment, or a jet reattached on either of the reservoir sidewalls. The results reveal also the occurrence of bi-stable flow configurations, i.e. different steady state flow fields are reached depending on the flow history. This is of high relevance for the design of shallow reservoirs as such configurations should certainly be avoided to achieve a robust hydraulic sizing of the reservoir.

Keywords: flow stability; hydrodynamic modelling; reattachment length; shallow reservoir; velocity field.

1. Introduction

Shallow reservoirs are common hydraulic structures. Their horizontal dimensions greatly exceed the vertical one, leading to predominantly two-dimensional flow. They are used as urban storm water retention ponds (Dominic, Aris, Sulaiman, & Tahir, 2016; Sebastian, Becouze-Lareure, Lipeme Kouyi, & Barraud, 2014), as storage reservoirs (Adamsson, Stovin, & Bergdahl, 2003; Michalec, 2015; Tsavdaris, Mitchell, & Williams, 2015), as sedimentation tanks (Liu, Xue, Hua, Yao, & Hu, 2013; Tarpagkou & Pantokratoras, 2013), as service reservoirs in water supply systems (Zhang et al., 2014), as well as in aquaculture (Persson & Wittgren, 2003; Persson, 2000). Complex flow develop in shallow reservoirs, involving large-scale horizontal coherent structures responsible for momentum transfers. These flow characteristics have a strong influence on processes such as contaminant and sediment transport (e.g., Saul & Ellis, 1992; Sloff, Jagers, & Kitamura, 2004). Therefore, predicting the flow field in shallow reservoirs is of critical importance for multiple engineering analyses, such as estimating the reservoir trapping efficiency (Adamsson et al., 2003; Dufresne, Dewals, Erpicum, Archambeau, & Pirotton, 2010a; Dufresne, Vazquez, Terfous, Ghenaim, & Poulet, 2009; Kantoush, 2008), or evaluating the water residence time for water quality assessment (Zhang et al., 2014).

A broad range of man-made shallow reservoirs have a rectangular or nearly-rectangular shape (Dufresne et al., 2009; Liu et al., 2013; Tarpagkou & Pantokratoras, 2013; Zhang et al., 2014). The flow field in rectangular shallow reservoirs was studied experimentally by Kantoush (2008), Dufresne, Dewals, Erpicum, Archambeau, & Pirotton (2010b), Camnasio, Orsi, & Schleiss (2011) and Choufi, Kettab, & Schleiss (2014), among others. Computational fluid dynamics is another proven technique for predicting and analysing the flow field in such structures (Dufresne et al., 2009; Tarpagkou & Pantokratoras, 2013; Tsavdaris et al., 2015; Yan et al., 2014; Zhang et al., 2014). For

rectangular shallow reservoirs, numerical studies were conducted by Kantoush, Bollaert, & Schleiss (2008), Dufresne, Dewals, Erpicum, Archambeau, & Pirotton (2011), Peng, Zhou, & Burrows (2012), Camnasio, Erpicum, Archambeau, Pirotton, & Dewals (2014), Secher, Hervouet, Tassi, Valette, & Villaret (2014) and Peltier, Erpicum, Archambeau, Pirotton, & Dewals (2015). A theoretical approach based on thermodynamic optimality was presented recently by Westhoff, Erpicum, Archambeau, Pirotton, & Dewals (2017).

As revealed in these studies, complex flow patterns were observed in rectangular shallow reservoirs, despite the simple geometry of the structure. Depending on the reservoir size and on the hydraulic boundary conditions, the flow fields involve either no flow reattachment or a jet with one or multiple reattachment points (Camnasio et al., 2011; Dufresne et al., 2010b). As a result of hydrodynamic instabilities, meandering jets were also observed as detailed in the flow typology presented by Peltier, Erpicum, Archambeau, Pirotton, & Dewals (2014).

Another peculiarity of flows in rectangular shallow reservoirs is the existence of bi-stable flow configurations. This was reported based on laboratory experiments, in which the flow switched randomly from one flow pattern to another (e.g., with and without reattachment) and vice-versa (Camnasio et al., 2011; Dufresne et al., 2010b). Such hydrodynamic instabilities are observed in geometric configurations corresponding to a so-called *transition zone*, in which the flow pattern shows a high sensitivity to small disturbances (Camnasio et al., 2011). In numerical studies, bi-stable flow configurations were identified as those leading to a different steady-state flow field depending on the initial condition prescribed in the numerical model (Dewals, Erpicum, Archambeau, & Pirotton, 2012; Dufresne et al., 2011).

Virtually all existing studies on rectangular shallow reservoirs focused solely on geometric setups in which the inlet and the outlet are situated along the reservoir centreline. However, as emphasized by Persson (2000), the locations of the inlet and outlet have a considerable impact on the hydraulic performance of the reservoir. Therefore, considering layouts involving inlet and outlet channels not aligned with the reservoir centreline is also of engineering relevance. So far, only Camnasio et al. (2013) considered inlet and outlet channels not aligned with the reservoir centreline; however, they analysed only three specific geometries. Though, their findings hint on the possible existence of bi-stable flow configurations as in one of their setups (labelled C-R in Camnasio et al. (2013)) the flow shifted from a reattached jet to a flow without reattachment as a result of a small disturbance (sediment deposits over a thickness of a few percent of the water depth).

In this paper, we use a validated numerical model to perform a first systematic analysis of the influence of the position of the inlet and outlet channels on the flow field in rectangular shallow reservoirs characterized by different length-to-width ratios. We consider only reservoirs with a single inlet and a single outlet. The results reveal the existence of sudden transitions between different flow patterns and the occurrence of bi-stable flow configurations.

In section 2, we briefly introduce the numerical model and we detail the considered reservoir geometries, the boundary conditions and the modelling procedure. The results are presented and discussed in section 3, while conclusions are drawn in section 4.

2. Method

2.1. Numerical model

The numerical simulations were performed with the academic flow model WOLF 2D, which solves the shallow-water equations by means of a second-order accurate finite volume scheme applied on a Cartesian grid. The turbulence closure used is a two-length-scale depth-averaged k–ε turbulence model as described by Erpicum, Meile, Dewals, Pirotton, & Schleiss (2009). The validity of this model for accurately predicting flow fields in shallow reservoirs was proven in several previous studies (Camnasio et al., 2013, 2014; Dufresne et al., 2011; Peltier et al., 2015).

2.2. Reservoir geometries

Apart from the location of the inlet and outlet channels, the reservoir characteristics and hydraulic conditions were the same as those tested experimentally by Camnasio et al. (2011). The reservoir bottom is smooth and horizontal, while the width of the inlet and outlet channels is equal to b = 0.25 m (Fig. 1). In all simulations, the reservoir width was kept constant (B = 4 m), while three different reservoir lengths were considered (L = 4.5 m, 5.5 m and 6 m). These three values were selected because, for a reservoir with the inlet and outlet channels along the centreline, experiments suggest that they lead to a straight jet, a transitional flow pattern and a reattached jet, respectively (Camnasio et al., 2011).

The inlet channel offset d_{in} is defined as the distance between the reservoir centreline and the inlet channel centreline, while the outlet channel offset d_{out} is measured between the reservoir centreline and the outlet channel centreline (Fig. 1). A positive (resp. negative) sign is assigned to d_{in} and d_{out} if the corresponding channel is located on the right (resp. left) side of the reservoir when looking streamwise.

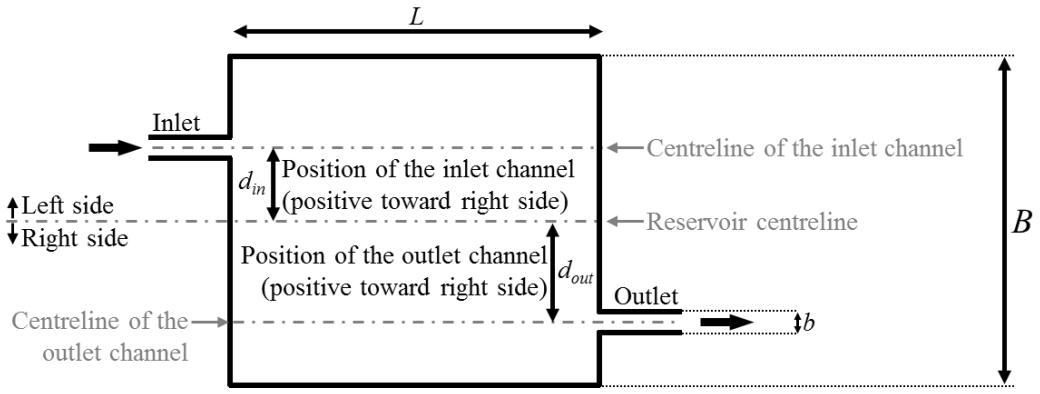

Figure 1 Sketch of a rectangular shallow reservoir (plane view), highlighting the relative positions d_{in} and d_{out} of the inlet and outlet channels with respect to the reservoir centreline.

2.3. Boundary conditions and discretization

Consistently with Camnasio et al. (2011), a constant inflow discharge Q = 0.7 l/s was prescribed as upstream boundary condition and the water depth was set to h = 0.2 m at the downstream end of the outlet channel. The corresponding inlet Froude number is $\mathrm{F} = Q / (b\, g^{1/2}\, h^{3/2}) \approx 0.1$.

The grid spacing is 0.025 m, which is consistent with the results of the grid convergence analysis presented by Dufresne et al. (2011) and is also equal to the grid spacing used by Camnasio et al. (2013). The adaptive time step is controlled by the Courant-Friedrichs-Lewy (CFL) condition (CFL = 0.5). It takes values of the order of 10^{-2} s. All simulations were run until a steady state was reached, as no meandering jet was observed in the considered configurations.

2.4. Simulation procedure

As highlighted in previous research (Dewals et al., 2012; Dufresne et al., 2011), the computed steady flow in rectangular shallow reservoirs may depend on the initial condition used for running the simulation. To investigate this issue, we followed here a two-step procedure for each considered geometry: a first simulation was conducted using water at rest as initial condition (step 1); next, a second simulation was run with a reattached jet as initial condition (step 2). This procedure is identical to the approach followed by Dewals et al. (2012). As a result, we could identify three types of configurations as a function of the computed flow fields:

- either the computed flow is reattached whatever the initial conditions;
- or the computed flow field corresponds to a jet flowing directly from the inlet to the outlet channel (no reattachment), whatever the initial conditions;
- or the flow is either reattached or not, depending on the initial conditions (bi-stable flow).

In this paper, we tested 11 different locations of the inlet channel along the reservoir upstream face, with varying positions of the outlet channel along the reservoir downstream face. This

led to roughly 60 different configurations for each reservoir length. Considering our two-step simulation procedure and by targeting the configurations of interest for capturing the transitions between the different flow patterns, we ended up with a total of about 280 numerical simulations.

3. Results and discussion

We detail in section 3.1 the results obtained when using water at rest as initial condition (step 1 of the simulation procedure). Next, by varying the initial conditions, we analyse the influence of flow history on the computed steady flow field and we highlight the occurrence of bi-stable flow configurations (section 3.2). The computed flow fields for all tested configurations are provided as online supplemental material (Fig. S1).

3.1. Flow patterns

Figure 2 indicates the type of computed flow pattern as a function of the location of the inlet and outlet channels for reservoirs of 4.5, 5.5 and 6 m in length. The *x*-axis in the plots of Fig. 2 represents the inlet channel offset d_{in}, while the *y*-axis indicates the outlet channel offset d_{out} (Fig. 1).

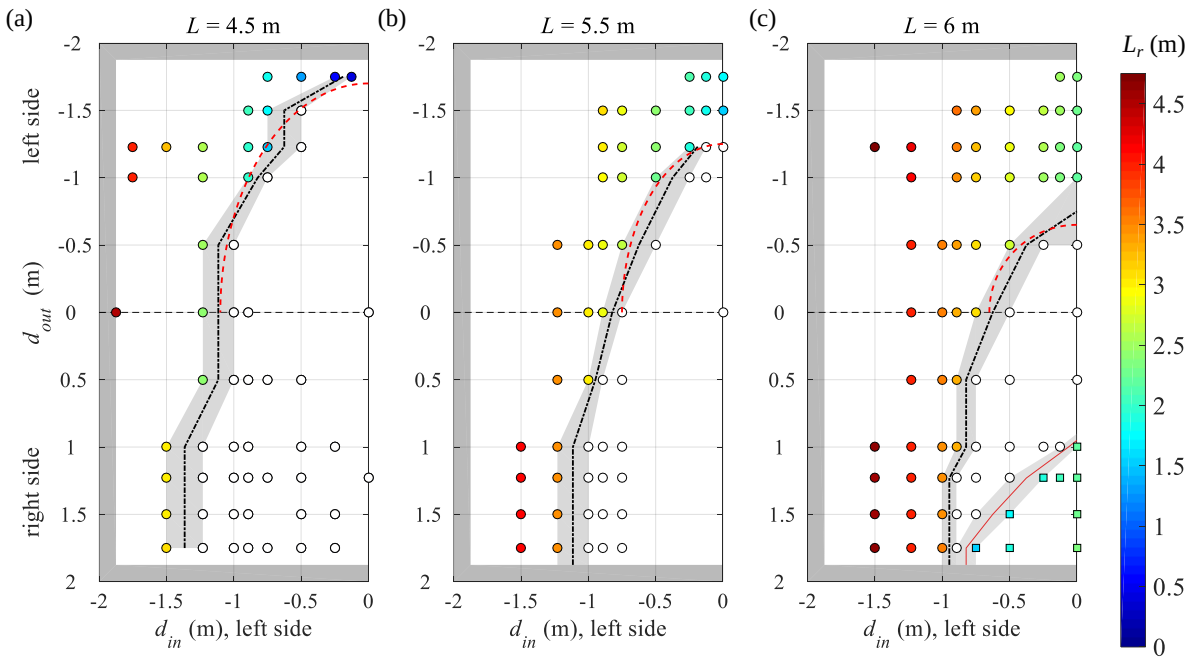

Figure 2 Type of computed flow pattern (symbols) and strength of reattachment if any (colour scale, in m), as a function of the locations d_{in} and d_{out} of the inlet and outlet channels for (a) a 4.5 m-long, (b) a 5.5 m-long and (c) a 6 m-long reservoir. Plain circles, empty circles and plain squares refer respectively to a left reattachment, no reattachment and a right reattachment. Initial condition: water at rest.

Due to symmetry, the inlet channel location was varied only toward one side of the reservoir (left side, i.e. $d_{in} \leq 0$). The dark grey shaded area along the sides of the plots has a thickness equal to

half the channels width and corresponds to an inaccessible region due to obvious geometric constraints.

The markers shape in Fig. 2 refers to three types of flow patterns: flow with reattached jet on the left sidewall (plain circles in Fig. 2), flow without reattachment (empty circles in Fig. 2), flow with reattached jet on the right sidewall (plain squares in Fig. 2c).The first two flow patterns are exemplified in Fig. 3a and 3b, respectively.

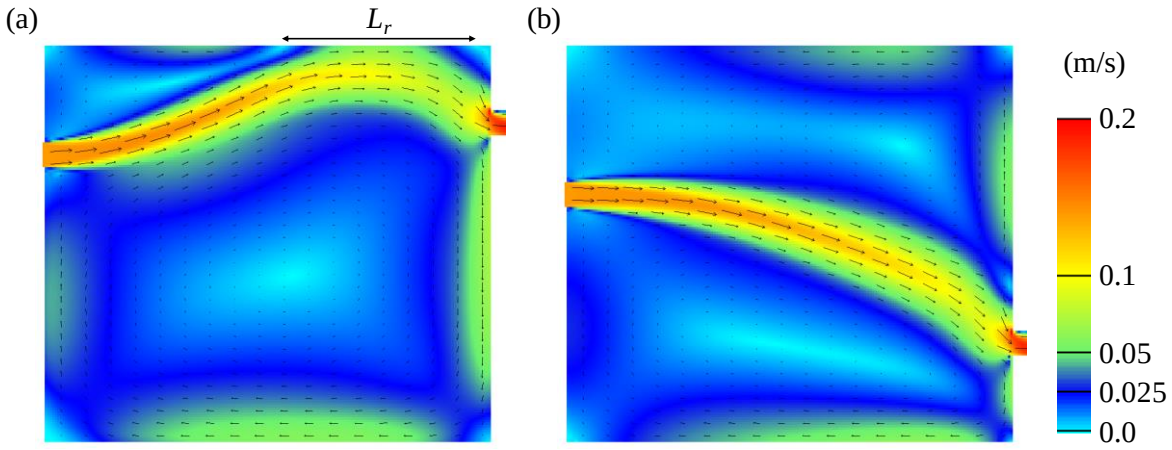

Figure 3 Computed flow fields (m/s) for two geometric configurations, leading respectively (a) to a reattached jet (L = 4.5 m, d_{in} = - 0.895 m and d_{out} = - 1.23 m) and (b) to a flow without reattachment (L = 4.5 m, d_{in} = - 0.5 m and d_{out} = 1 m). Notation L_r refers to the length over which the jet remains reattached to the sidewall (reattachment strength).

The markers colour in Fig. 2 indicates the *strength* of the reattachment, expressed as the length L_r over which the jet remains attached to the sidewall (Fig. 3). The dashed broken lines delineate the limits between regions of the plot corresponding to different types of flow patterns; and the light grey shaded areas show the uncertainty on these limits, which could be reduced by simply running more simulations.

When the inlet and outlet channels are both located on the *same* side of the reservoir centreline, the locations of both channels have a substantial influence on the type of flow pattern (upper part of the plots in Fig. 2). The threshold between the two types of flow patterns may be described approximately by an elliptical boundary (red dashed lines in Fig. 2):

$$(\alpha\, d_{in}/B)^2 + (\beta\, d_{out}/B)^2 = 1, \qquad (1)$$

with α and β adjusted separately for each reservoir length, as detailed in Tab. 1.

Table 1 Adjusted parameters α and β in Eq. (1) describing the threshold between flow patterns with and without reattachment when the inlet and outlet channels are located on the same side of the reservoir centreline.

L	4.5	5.5	6.0
α	0.28	0.19	0.16
β	0.43	0.31	0.16

For the longer reservoirs (L = 5.5 m and L = 6 m), a reattached flow can even be obtained when the inlet channel is aligned with the reservoir centreline (d_{in} = 0), provided that the outlet channel is located far enough from the reservoir centreline ($|d_{out}| > 0.6\ B / 2$ and $0.4\ B / 2$ for L = 5.5 m and L = 6 m, respectively).

Contrarily to the case when the inlet and outlet channels are situated on the same side of the reservoir centreline, when they are on *either side* of the reservoir centreline, the transition between ″reattachment on the sidewall closer to the inlet channel″ and ″no reattachment″ is primarily controlled by the location of the inlet channel itself. This is shown by the quasi-vertical transition line in the lower part of the plots in Fig. 2, reflecting the quasi-independence of the threshold from d_{out}. For the longer reservoirs (Figs. 2b and 2c), the computed jet is reattached on the wall closer to the inlet channel, if the distance between the inlet channel centreline and the reservoir centreline exceeds roughly one half of the reservoir half-width ($|d_{in}| \geq B / 4$). For the shortest reservoir (Fig. 2a), this threshold is shifted to about three quarters of the reservoir half-width ($|d_{in}| \geq 3\ B / 8$). Otherwise, the computed flow field shows no reattachment, except in the case of the longest reservoir, for which a reattachment on the sidewall opposite to the inlet channel is found when $d_{in} + d_{out}$ exceeds about $B / 4$ (red broken line in Fig. 2c). In the latter case, the reattachment strength remains relatively weak compared to cases in which the jet reattaches to the sidewall closer to the inlet channel. Note that the results corresponding to the inlet channel along the reservoir centreline (d_{in} = 0) are symmetric in the upper and lower parts of Fig. 2. Although it was not investigated explicitly, a jet reattachment on the sidewall opposite to the inlet channel also occurs in the case of the reservoir length of 5.5 m, due to symmetry reasons.

In all cases, the colour of the markers reveals that the strength of reattachment L_r depends primarily on the location of the inlet channel.

3.2. Bi-stable flow configurations

The results of sect. 3.1 were all obtained from an initial condition without reattachment (water at rest). To appreciate the stability of the computed flow patterns which do not display flow reattachment, the simulations were repeated starting from an initial condition with flow reattachment (step 2 of the simulation procedure). We consider these flow patterns as stable if they remain

unchanged even when the simulation is started from a different initial condition, i.e. with reattachment. In contrast, *bi-stable* flow configurations refer to those in which a different flow pattern is obtained depending on the initial condition. These configurations are represented by diamond symbols in Fig. 4, which focuses on the occurrence and strength of flow reattachment only on the same side as the inlet channel. A new transition can be defined from the results in Fig. 4. It delineates the bi-stable flow configurations from those in which only a flow pattern without reattachment is stable (dotted lines in the plots in Fig. 4). This transition corresponds mostly to a vertical line (d_{in} = cst) and the corresponding threshold value on $|d_{in}|$ gradually decreases from about B / 4 for L = 4.5 m to approximately zero for L = 6 m.

The presence of two distinct transitions reveals the existence of a hysteresis effect in the change of flow pattern when the location of the inlet and outlet channels are varied, as discussed previously by Dewals et al. (2012) for inlet and outlet channels located along the reservoir centreline. This effect is particularly present when the inlet and outlet channels are located on either sides of the reservoir centreline. The distance between the two transitions (dashed and dotted broken lines in Fig. 4) reflects the magnitude of the hysteresis effect, which rises gradually as the reservoir length is increased.

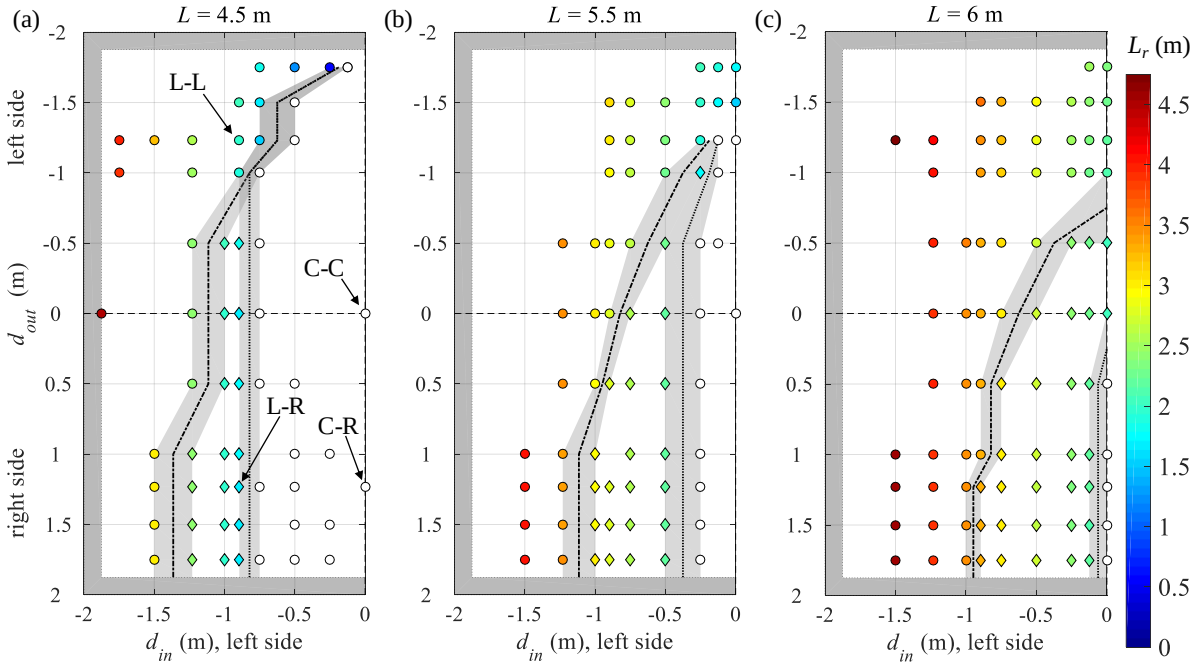

Figure 4 Type of computed flow pattern (symbols) and strength of reattachment if any (colour scale, in m), as a function of the locations d_{in} and d_{out} of the inlet and outlet channels for (a) a 4.5 m-long, (b) a 5.5 m-long and (c) a 6 m-long reservoir. Plain circles, empty circles and plain diamonds refer respectively to a left reattached flow, a flow without left reattachment and a bi-stable flow configuration. Initial condition: reattached flow. Labels C-C, L-L, L-R and C-R in panel (a) refer to the configurations tested by Camnasio et al. (2013).

The present results are consistent with the experimental observations of Camnasio et al.

(2013) for L = 4.5 m. The configurations tested by Camnasio et al. (2013) are indicated by labels in Fig. 4a (C-C, L-L, C-R and L-R). As experimentally observed, the computed flow fields show no reattachment for configurations C-C and C-R, while the computed jet is reattached on the left side-wall in configuration L-L (Fig. S1a in supplemental online material). For test L-R, the computational results obtained herein shed new light on the findings of Camnasio et al. (2013). Indeed, in the experiments, the flow in test L-R was reattached; but it switched to a flow without reattachment as soon as a limited amount of sediment deposits accumulated on the reservoir bottom. Here, the computations reveal that test L-R corresponds to a bi-stable flow configuration (Fig. 4a) and is very close to the region of no flow reattachment. This result matches the observed high sensitivity of the flow field with respect to an external disturbance (limited sediment deposits), as reported by Camnasio et al. (2013), and its tendency to shift to a flow pattern without reattachment.

4. Conclusion

Based on a validated numerical model, we systematically analysed how the inlet and outlet channels locations in rectangular shallow reservoirs influence the occurrence of flow reattachment on the reservoir sidewalls.

When the inlet and outlet channels are located on opposite sides of the reservoir centreline, the flow pattern is mainly controlled by the inlet channel. For the tested configurations, the transition between a reattached jet and no reattachment was obtained for a distance between the inlet channel centreline and the reservoir centreline between one half (longer reservoirs) and three quarters (shortest reservoir) of the reservoir width. In contrast, when the inlet and outlet channels are situated on the same side of the reservoir centreline, the locations of both channels have an influence of similar importance on the flow pattern.

We used a tailored two-step modelling procedure, involving two runs starting from different initial conditions, to highlight the existence of geometric configurations leading to bi-stable flow conditions. The flow history was shown to have a growing influence when the length-to-width ratio of the reservoir is increased. The obtained results are in agreement with previous experimental observations by Camnasio et al. (2013), and they also provide additional clues for a deeper understanding of these earlier observations.

The presented results are of relevance to inform the engineering design and the operation of shallow reservoirs in several aspects.

- First, the awareness of the existence of bi-stable flow configurations should help designers to avoid these configurations, since a structure in which the flow pattern changes randomly would fail to comply with predefined performance criteria. In this respect, the diagrams provided in Fig. 4 are particularly helpful to identify the combinations of geometric parameters (L, d_{in}, d_{out}) leading to bi-stable flow configurations.

- Second, Dufresne et al. (2010a) showed that sedimentation rates are substantially higher when the flow reattaches to a reservoir sidewall. Hence, the results displayed in Fig. 4 may contribute to identify reservoir geometries which promote flow reattachment for the design of sedimentation tanks (coloured markers in Fig. 4), and vice-versa in the case of water storage reservoirs (empty markers in Fig. 4).
- Since flow reattachment tends to also increase the water age and residence time, similar considerations as for sedimentation apply for the design of structures in which water age and residence time are important parameters in terms of water quality (Zhang et al., 2014). For instance, if the design aims at obtaining a reattached flow field, Fig. 4 reveals that considering $d_{in} \leq - 3 / 8\ B$ is a robust choice for the three tested reservoir lengths.

Another implication of broad interest

Another implication of the study is that it emphasizes the need for performing sensitivity analysis with respect to the initial conditions (besides model parameters and input data) whenever a hydraulic structure is designed based on numerical simulations. This is indeed the most straightforward way to identify the occurrence of bi-stable flow configurations.

The main limitations of the present study include the consideration of a single set of hydraulic boundary conditions, as well as uncertainties arising from the numerical model. Indeed, although the model was shown to predict accurately the velocity profiles for a given flow pattern (Camnasio et al., 2013, 2014), capturing the exact threshold conditions between two different flow patterns may be more challenging. In this regard, the performance of alternate turbulence closures and 3D models should be investigated in further research. Another valuable contribution would be the use of a morphodynamic model to figure out the influence of the inlet and outlet locations on the pattern of sediment deposits and its feedback on the flow field. To some extent, the findings of the present study could also be extrapolated to other fields of fluid mechanics, in which sudden enlargements play a central part such as studies on the influence of buildings on exposure to air pollution (Ng & Chau, 2014).

Acknowledgements

N/A

Funding

N/A

Supplemental data

All computed flow fields are displayed in Fig. S1 provided as online supplemental material.

Notation

b = width of the inlet and outlet channels (m)

B = reservoir width (m)

d_{in} (resp. d_{out}) = distance between the reservoir centreline and the inlet (resp. outlet) channel centreline (m)

F = inlet Froude number (-)

g = gravity acceleration (ms^{-2})

h = water depth (m)

L = reservoir length (m)

L_r = length over which the jet is reattached to the reservoir sidewall (m)

Q = water discharge (m^3s^{-1})

x = streamwise coordinate (m)

y = transverse coordinate (m)

α, β = regression coefficients (-)

References

Adamsson, Ã., Stovin, V., & Bergdahl, L. (2003). Bed shear stress boundary condition for storage tank sedimentation. *Journal of Environmental Engineering, 129*(7), 651–658.

Camnasio, E., Erpicum, S., Archambeau, P., Pirotton, M., & Dewals, B. (2014). Prediction of mean and turbulent kinetic energy in rectangular shallow reservoirs. *Engineering Applications of Computational Fluid Mechanics, 8*(4), 586–597.

Camnasio, E., Erpicum, S., Orsi, E., Pirotton, M., Schleiss, A. J., & Dewals, B. (2013). Coupling between flow and sediment deposition in rectangular shallow reservoirs. *Journal of Hydraulic Research, 51*(5), 535–547.

Camnasio, E., Orsi, E., & Schleiss, A. (2011). Experimental study of velocity fields in rectangular shallow reservoirs. *Journal of Hydraulic Research, 49*(3), 352–358.

Choufi, L., Kettab, A., & Schleiss, A. J. (2014). Bed roughness effect on flow field in rectangular shallow reservoir [Effet de la rugosité du fond d′un réservoir rectangulaire à faible profondeur sur le champ d′écoulement]. *Houille Blanche*, (5), 83–92.

Dewals, B., Erpicum, S., Archambeau, P., & Pirotton, M. (2012). Discussion of ″Experimental study of velocity fields in rectangular shallow reservoirs. *Journal of Hydraulic Research, 50*(4), 435−436.

Dominic, J. A., Aris, A. Z., Sulaiman, W. N. A., & Tahir, W. Z. W. M. (2016). Discriminant analysis for the prediction of sand mass distribution in an urban stormwater holding pond using simulated depth average flow velocity data. *Environmental Monitoring and Assessment*, *188*(3), 1−15.

Dufresne, M., Dewals, B. J., Erpicum, S., Archambeau, P., & Pirotton, M. (2010a). Experimental investigation of flow pattern and sediment deposition in rectangular shallow reservoirs. *International Journal of Sediment Research*, *25*(3), 258−270.

Dufresne, M., Dewals, B. J., Erpicum, S., Archambeau, P., & Pirotton, M. (2010b). Classification of flow patterns in rectangular shallow reservoirs. *Journal of Hydraulic Research*, *48*(2), 197−204.

Dufresne, M., Dewals, B. J., Erpicum, S., Archambeau, P., & Pirotton, M. (2011). Numerical investigation of flow patterns in rectangular shallow reservoirs. *Engineering Applications of Computational Fluid Mechanics*, *5*(2), 247−258.

Dufresne, M., Vazquez, J., Terfous, A., Ghenaim, A., & Poulet, J.-B. (2009). CFD modeling of solid separation in three combined sewer overflow chambers. *Journal of Environmental Engineering*, *135*(9), 776−787.

Erpicum, S., Meile, T., Dewals, B. J., Pirotton, M., & Schleiss, A. J. (2009). 2D numerical flow modelling in a macro-rough channel. *International Journal for Numerical Methods in Fluids*, *61*(11), 1227−1246.

Kantoush, S. A. (2008). *Experimental study on the influence of the geometry of shallow reservoirs on flow patterns and sedimentation by suspended sediments*. EPFL, Lausanne, Switzerland.

Kantoush, S. A., Bollaert, E., & Schleiss, A. J. (2008). Experimental and numerical modelling of sedimentation in a rectangular shallow basin. *International Journal of Sediment Research*, *23*(3), 212−232.

Liu, X., Xue, H., Hua, Z., Yao, Q., & Hu, J. (2013). Inverse calculation model for optimal design of rectangular sedimentation tanks. *Journal of Environmental Engineering (United States)*, *139*(3), 455−459.

Michalec, B. (2015). Evaluation of an empirical reservoir shape function to define sediment distributions in small reservoirs. *Water (Switzerland)*, *7*(8), 4409−4426.

Ng, W.-Y., & Chau, C.-K. (2014). A modeling investigation of the impact of street and building configurations on personal air pollutant exposure in isolated deep urban canyons. *Science of the Total Environment*, *468-469*, 429−448.

Peltier, Y., Erpicum, S., Archambeau, P., Pirotton, M., & Dewals, B. (2014). Experimental investigation of meandering jets in shallow reservoirs. *Environmental Fluid Mechanics*, *14*(3), 699−710.

Peltier, Y., Erpicum, S., Archambeau, P., Pirotton, M., & Dewals, B. (2015). Can meandering flows in shallow rectangular reservoirs be modeled with the 2D shallow water equations? *Journal of Hydraulic Engineering*, *141*(6).

Peng, Y., Zhou, J. G., & Burrows, R. (2012). Modeling free-surface flow in rectangular shallow basins by using lattice boltzmann method. *Journal of Hydraulic Engineering*, *137*(12), 1680−1685.

Persson, J. (2000). The hydraulic performance of ponds of various layouts. *Urban Water Journal*, *2*(3), 243−250.

Persson, J., & Wittgren, H. B. (2003). How hydrological and hydraulic conditions affect performance of ponds. *Ecological Engineering*, *21*(4-5), 259−269.

Saul, A.J., Ellis, D.R. (1992). Sediment deposition in storage tanks. *Water Science and Technology* 25(8), 189−198.

Sebastian, C., Becouze-Lareure, C., Lipeme Kouyi, G., & Barraud, S. (2014). Event-based quantification of emerging pollutant removal for an open stormwater retention basin - Loads, efficiency and importance of uncertainties. *Water Research*, *72*, 239−250.

Secher, M., Hervouet, J.-M., Tassi, P., Valette, E., & Villaret, C. (2014). Numerical Modelling of Two-Dimensional Flow Patterns in Shallow Rectangular Basins. In P. Gourbesville, J. Cunge, & G. Caignaert (Eds.), Advances in Hydroinformatics (pp. 499−510). Springer.

Sloff, C.J., Jagers, H.R.A., Kitamura, Y. (2004). Study on the channel development in a wide reservoir. *Proc. River Flow*, Napoli, Italy, pp. 811-819.

Tarpagkou, R., & Pantokratoras, A. (2013). CFD methodology for sedimentation tanks: The effect of secondary phase on fluid phase using DPM coupled calculations. *Applied Mathematical Modelling*, *37*(5), 3478−3494.

Tsavdaris, A., Mitchell, S., & Williams, J. B. (2015). Computational fluid dynamics modelling of different detention pond configurations in the interest of sustainable flow regimes and gravity sedimentation potential. *Water and Environment Journal*, *29*(1), 129−139.

Westhoff, M., Erpicum, S., Archambeau, P., Pirotton, M., & Dewals, B. (2017). Maximum energy dissipation to explain velocity fields in shallow reservoirs. *Journal of Hydraulic Research, in press*.

Yan, H., Lipeme Kouyi, G., Gonzalez-Merchan, C., Becouze-Lareure, C., Sebastian, C., Barraud, S., & Bertrand-Krajewski, J.-L. (2014). Computational fluid dynamics modelling of flow and particulate contaminants sedimentation in an urban stormwater detention and settling basin. *Environmental Science and Pollution Research*, *21*(8), 5347−5356.

Zhang, J.-M., Lee, H. P., Khoo, B. C., Peng, K. Q., Zhong, L., Kang, C.-W., & Ba, T. (2014). Shape effect on mixing and age distributions in service reservoirs. *Journal - American Water Works Association*, *106*(11), E481−E491.